Flow-through comb electroporation device for delivery of macromolecules

Andrea Adamo[#], **Alessandro Arione**[#,†], **Armon Sharei**, and **Klavs F. Jensen**[*]
Department of Chemical Engineering, Massachusetts Institute of Technology, 77 Massachusetts Avenue, Cambridge, MA 02139, USA

Abstract

We present a microfluidic electroporation device with a comb electrode layout fabricated in polydimethylsiloxane (PMDS) and glass. Characterization experiments with HeLa cells and fluorescent dextran show efficient delivery (~95%) with low toxicity (cell viability ~85%) as well as rapid pore closure after electroporation. The activity of delivered molecules is also verified by silencing RNA (siRNA) studies that demonstrate gene knockdown in GFP expressing cells. This simple, scalable approach to microfluidic, flow-through electroporation could facilitate the integration of electroporation modules within cell analysis devices that perform multiple operations.

Introduction

Electroporation is used for the delivery of a variety of cell-impermeable molecules such as DNA, RNA, drugs, antibodies, and dyes into mammalian cells.[1, 2] Its popularity stems mainly from its versatility and simplicity. Cell electroporation occurs once the transmembrane potential exceeds a critical threshold value. The transmembrane potential depends, among other things, on the electric field around the cell.[3] The small size of microfluidic-based systems provides the advantage of lowering the voltages needed to generate critical electric fields, since the length scale is generally reduced. That platform has additional advantages including,[4] the ability to form uniform or symmetrical electric fields, the capability to generate controlled conditions, the potential for rapid optimization of delivery protocols, and the more efficient (cost-saving) use of reagents. Moreover, integration of electroporation into micro total analysis systems could open up the possibility of new applications.[5]

In the last decade, a number of microfluidic flow-through electroporation systems for the delivery of molecules into mammalian cells have been described. For example, some systems vary channel width to concentrate the electric field,[6, 7] while different channel lengths have been used to facilitate rapid optimization of delivery conditions.[8] To reduce the applied voltage and eliminate bubbles, channels with polyelectrolytic gel electrodes [9] and serpentine aluminum channels have also been suggested.[10, 11] Other work has demonstrated electric field pulsation with DC power supplies[12] to simplify the experimental setup and laminar flow focusing of cell suspension with stream of buffer solution[13] to minimize reactions at the electrodes and pH change. Finally, AC electric fields have been used to eliminate bubble formation.[14]

[*]Corresponding author kfjensen@mit.edu.
[#]These authors contributed equally to the paper
[†]Current address Politecnico di Torino, Department of electronic engineering, Corso Duca degli Abruzzi 24, 10129 Torino, ITALY

While progress has been made in the field of flow-through electroporation systems, a design that is easy to operate, fabricate and integrate within more complex chips has yet to be described.[15] In this work, we address this challenge with a "comb type" design of the electrode pattern that, coupled with the use of AC voltages and appropriate channel size, provides bubble-free, localized electroporation as well as high cell viability. The design and its operating conditions minimize the voltage required for operation and allow for miniaturization of the device by eliminating the need for large area electrodes. After exploring the behavior of the chip, by delivering cell-impermeable dextran conjugated dyes, we demonstrate successful delivery of a cell-impermeable actin stain for live cell analysis and delivery of siRNA.

Microfluidic chip design and fabrication

The main idea behind the chip design is to use an interdigitated electrode pattern deposited on one side of the cell flow channel. The electrodes can be placed at a reduced distance in order to minimize the voltage required to create fields adequate for cell poration. In order to have an essentially uniform electric field between the electrodes, the distance of the electrodes has to be larger than the height of the channel. The channel width can be freely selected. The electrodes are powered by a high frequency AC voltage to avoid bubble formation at the electrodes.

To implement the above device concept, a polydimetylsiloxane (PDMS) (Dow Corning, USA) chip (Figure1) with a straight channel was bonded to Borofloat glass with gold electrodes patterned onto it using lift off. The channel was 50 μm wide and 15 μm high. The gold electrodes were 25 μm wide, 75 μm apart and 100 nm thick. Once a cell travelling through the channel reaches the area containing the electrodes, it is subjected to an electric field. In order to simplify the study of the role of cell exposure time to the electric field, we built sets of electrodes with different sizes onto each chip. By changing which electrode set is being used, we would change the cell's exposure time. We built three sets of electrodes with 10, 20 and 30 electrode couples corresponding to a channel length of 750, 1500 and 2250 μm respectively. The chips had contact pads for connection to a function generator (Agilent). We also included additional electrodes as probes for in situ measurement of the local fields. A multi-physics simulation (COMSOL Multiphysics) simulation (Figure 2) confirmed that the field between the electrodes is essentially constant. The simulation also showed that above each electrode there is a point with a null field. Thus, as a cell travels through the channel it experiences both a field variation due to the externally imposed AC voltage and due to the field variation along the channel. The timescales of the two variations are very different with the one due to the external voltage being orders of magnitude faster than the one defined by electrode spacing.

The channel height (15μm) just larger than the typical cell diameter (~10–12μm) ensures flow of the cells leaving them an almost obligated passage. We expect the vertical position of the cell to play a limited role out of the uniformity of the electric field.

Experimental procedures

The experimental set up included the microfluidic chip powered by a function generator producing a sine wave at 100 kHz with amplitudes in the range of 4–7 V. Lower amplitudes gave fields too weak for electroporation and larger ones resulted in rapid degradation of the electrodes. The corresponding electric fields were in the 16–28 kV/m range, as measured with the probe electrodes.

An operating frequency of 100 kHz was selected so that we could neglect the loss in impedance due to double layer capacitance.[16, 17] Typical double layer capacitance is 15

μFcm^2.[18] Thus, at f=100 kHz, the capacitive impedance of an electrode is $1/(2\omega f^*C) \sim 10^4 \Omega$ (with C being the double layer capacitance of one electrode). We assume this effect is negligible with respect to the resistive impedance ($\sim 10^5 \Omega$ in phosphate buffer solution) between two consecutive electrodes.

The flow of the cell suspension through the chip was pressure driven and controlled by a pressure regulator. Typical cell speeds were ~10 mm/s.

For each experiment, cultured HeLa cells were washed with PBS and then detached with trypsin (0.05%) for 10 min. The trypsin reaction was quenched by adding a volume of media equal to twice the volume of trypsin. Cells were then centrifuged, resuspended in a flow buffer composed of PBS containing 3 % bovine serum, 1% pluronics (F-68), and $CaCl_2$ (2 mg/ml), and flown through the chip.

Delivery of cell impermeable fluorescent dextran conjugates

In order to test the ability of the chip to deliver cell impermeable molecules, we selected a cell impermeable dextran conjugated to fluorescein (MW 10,000; Invitrogen). We tested the effect of electric fields with different strengths and different exposure times on cells. In each experiment, the cells were prepared as described above and the fluorescently-labeled dextran was added to the cell suspension before flowing it through the chip. Once the cells were collected from the chip, they were cultured for 18 hours and then stained with propidium iodide (50 μg/ml) as a test for viability and analyzed by flow cytometry (FACS LSR II-HTS, Becton Dickinson). Each experimental condition was repeated at least three times. For each experiment, the control was represented by cells flown through the chip in the absence of an applied electric field. During the course of our experiments, we observed a dependence of viability and delivery efficiency on the state of confluence of the cells. As a consequence, we standardized all of the experiments by utilizing cells within 48 hours of their most recent media change[19] at a cell density of ~80–100 cells/mm^2.

Phallotoxin experiments

We explored the delivery of phallotoxins to cells to demonstrate delivery of molecules other than dextran, Phallotoxins are used to stain actin[20,21] and are known to be cell impermeable.[22] Most often, they are used on fixed cells, but staining of live cells using lipotransfer-mediated delivery of phallotoxins has been reported.[22] To demonstrate phallotoxin delivery, we prepared the cells as described above and resuspended them in the flow buffer with 4.4 μM of phallacidin fluorescently labeled with Bodipy (B607, Invitrogen). Electroporation conditions were those that provided the highest yield in the dextran delivery experiments (exposure time=72 ms, field=24 kV/m). As a control, cells were flown through the chip in the absence of an electric field. Cells were then collected and placed in a chambered cover slip (Lab Tek, USA) and imaged using a confocal microscope (Zeiss Axiovert with a Perkin Elmer spinning disk confocal microscope).

Delivery of siRNA

Gene silencing experiments were also performed to assess the potential to use this system as a method for controlling gene expression.[23, 24] Stable GFP-expressing HeLa cells were electroporated in the presence of GFP silencing siRNA (Ambion) and analyzed by FACS (fluorescent activated cell sorting) (FACS Canto II, BD Biosciences) 48 hours after delivery for fluorescence knockdown (exposure time=72 ms, field=24 kV/m).

Results and discussion

Figure 3 shows the results of the dextran experiments in terms of delivery efficiency, cell viability and delivery yield. These quantities are plotted against field strength and exposure time as a parameter. Delivery efficiency, cell viability and delivery yield are defined as:[25]

$$\text{Delivery Efficiency}(\%) = (G/V) \times 100\% \quad (1)$$

$$\text{Cell Viability}(\%) = (V/T) \times 100\% \quad (2)$$

$$\text{Delivery Yield}(\%) = (G/T) \times 100\% \quad (3)$$

Here G=the number of cells containing the conjugated dextran, V=the number of viable cells (cells not stained by PI), and T=the total number of cells observed.

The data show that delivery efficiency increases with stronger fields and longer exposure times. In contrast, viability decreases in the presence of stronger fields and longer exposure times. As a result, the delivery yield exhibits a maximum for a set exposure time. In particular, the exposure time of 72 ms and 24 kV/m gives a delivery yield of 80% with ~92 % of cells delivered.

With an eye towards future integration of the electroporation chip with other cell microfluidic operations, it is useful to know how long the cells are able to uptake (or release) material from (or to) the surrounding environment. As a test, we compared the delivery efficiency in two different cases. In the first case, cells are electroporated in the channel with the dextran in the cell suspension as previously described, but the suspension medium is diluted once the cells arrived in the collection reservoir. In the second case, the cells are electroporated in a medium without any dye and the cells meet the dye in the collection reservoir (about 20 ms after the exposure to the electric field). In both cases electroporation exposure time to the electric field is 72 ms and the field intensity is 24 kV/m. In the first case the delivery efficiency is about 82% while in the latter case the delivery is about 2% (Figure 4). These results indicate that the pores are only open when the cells are exposed to the electric field and the pores are practically closed within 20 ms after the end of the electric field. As a note, typical fluid flow rates in the device are ~2ul/min, while the reservoir contains >20ul of solution (with or without dye). Collection occurred every minute, and experiments were repeated 3 times.

For electroporated cells, the Phallotoxin experiments resulted in stained actin[20,21] within the cells showing fluorescence at both the Bodipy (excitation/emission 505/512) and Cascade Blue wavelengths in confocal microscopy while control cells did not show evidence of either fluorophore. The dextran conjugated with the Cascade Blue is used to confirm that the cell has been succesfully electroporated. Figure 4 shows confocal images at different heights of a stained cell collected using a filterset adequate for the emission range of the Phallotoxin.

When GFP-expressing HeLa cells are electroporated in the presence of GFP silencing siRNA (Ambion.), knockdown of gene expression (decreased fluorescence) is observed at 48 hours after treatment. The concentration-dependent knockdown profile (p<0.001, analysis of variance (ANOVA) followed by Bonferroni post-hoc test) (Figure 5) demonstrates the system's ability to deliver bioactive materials to the cell cytosol and illustrates its potential for gene regulation. Delivery of scrambled siRNA controls did not

produce any gene knockdown thereby indicating that the electroporation process itself is not responsible for the observed results.

Conclusions

The present study has demonstrated a microfluidic-based electroporation device with a comb design electrode layout that with an applied AC electric field provided successful electroporation of HeLa cells. A 100 kHz operating frequency made the effect of double layer capacitance negligible, allowing for low operating voltages and electrode miniaturization. Electroporation performance was characterized by fluorescent dextran and showed a peak delivery yield of 82%. Additionally, cells exhibited a short pore closure time after electroporation. Delivery of cell-impermeable molecules into cells, specifically phallotoxin for actin staining and siRNA for gene knockdown, established the ability to deliver active materials into the cells during electroporation. This simple and scalable microfabrication approach to electroporation could be used for the integration of electroporation modules within complex devices that perform electroporation as one of many functions.
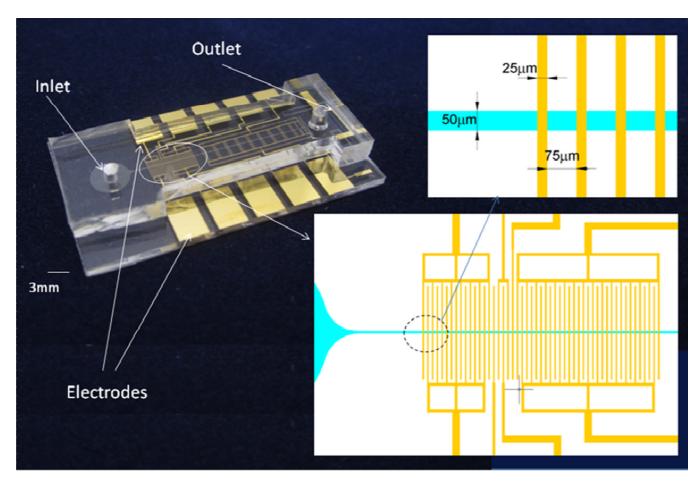
Acknowledgments

References

1. Neumann E, Kakorin S, Toensing K. Fundamentals of electroporative delivery of drugs and genes. Bioelectrochemistry and Bioenergetics. 1999; 48(1):3–16. [PubMed: 10228565]

2. Lambert H, Pankov R, Gauthier J, Hancock R. Electroporation-Mediated Uptake of Proteins into Mammalian-Cells. Biochemistry and Cell Biology-Biochimie Et Biologie Cellulaire. 1990; 68(4): 729–734. [PubMed: 2222997]

3. Weaver JC, Chizmadzhev YA. Theory of electroporation: A review. Bioelectrochemistry and Bioenergetics. 1996; 41(2):135–160.

4. Lee WG, Demirci U, Khademhosseini A. Microscale electroporation: challenges and perspectives for clinical applications. Integrative Biology. 2009; 1(3):242–251. [PubMed: 20023735]

5. Kim J, Hwang I, Britain D, Chung TD, Sun Y, Kim DH. Microfluidic approaches for gene delivery and gene therapy. Lab Chip. 11(23):3941–3948. [PubMed: 22027752]

6. Lu C, Wang HY. Electroporation of mammalian cells in a microfluidic channel with geometric variation. Analytical Chemistry. 2006; 78(14):5158–5164. [PubMed: 16841942]

7. Wang HY, Lu C. Microfluidic electroporation for delivery of small molecules and genes into cells using a common DC power supply. Biotechnol Bioeng. 2008; 100(3):579–586. [PubMed: 18183631]

8. Kim JA, Cho K, Shin YS, Jung N, Chung C, Chang JK. A multi-channel electroporation microchip for gene transfection in mammalian cells. Biosens Bioelectron. 2007; 22(12):3273–3277. [PubMed: 17395450]

9. Chung TD, Kim SK, Kim JY, Kim KP. Continuous low-voltage dc electroporation on a microfluidic chip with polyelectrolytic salt bridges. Analytical Chemistry. 2007; 79(20):7761–7766. [PubMed: 17874852]

10. Wang S, Zhang X, Wang W, Lee LJ. Semicontinuous flow electroporation chip for high-throughput transfection on mammalian cells. Anal Chem. 2009; 81(11):4414–4421. [PubMed: 19419195]

11. Wang S, Zhang X, Yu B, Lee RJ, Lee LJ. Targeted nanoparticles enhanced flow electroporation of antisense oligonucleotides in leukemia cells. Biosens Bioelectron. 26(2):778–783. [PubMed: 20630739]

12. Lu C, Wang J, Stine MJ. Microfluidic cell electroporation using a mechanical valve. Analytical Chemistry. 2007; 79(24):9584–9587. [PubMed: 18004820]

13. Du Q, Wei ZW, Zhao DY, Li XM, Wu MX, Wang W, Huang H, Wang XX, Liang ZC, Li ZH. A Laminar Flow Electroporation System for Efficient DNA and siRNA Delivery. Analytical Chemistry. 2011; 83(15):5881–5887. [PubMed: 21678996]

14. Gazit D, Ziv R, Steinhardt Y, Pelled G, Rubinsky B. Micro-electroporation of mesenchymal stem cells with alternating electrical current pulses. Biomedical Microdevices. 2009; 11(1):95–101. [PubMed: 18815886]

15. Li DQ, Movahed S. Microfluidics cell electroporation. Microfluidics and Nanofluidics. 2011; 10(4):703–734.

16. Gawad S, Schild L, Renaud P. Micromachined impedance spectroscopy flow cytometer for cell analysis and particle sizing. Lab on a Chip. 2001; 1(1):76–82. [PubMed: 15100895]

17. Bard, AJ.; Faulkner, LR. Electrochemical methods : fundamentals and applications. 2nd ed. New York: Wiley; 2001. p. xxi-833.

18. Gawad S, Cheung K, Seger U, Bertsch A, Renaud P. Dielectric spectroscopy in a micromachined flow cytometer: theoretical and practical considerations. Lab on a Chip. 2004; 4(3):241–251. [PubMed: 15159786]

19. Akinc A, Zumbuehl A, Goldberg M, Leshchiner ES, Busini V, Hossain N, Bacallado SA, Nguyen DN, Fuller J, Alvarez R, Borodovsky A, Borland T, Constien R, de Fougerolles A, Dorkin JR, Narayanannair Jayaprakash K, Jayaraman M, John M, Koteliansky V, Manoharan M, Nechev L, Qin J, Racie T, Raitcheva D, Rajeev KG, Sah DW, Soutschek J, Toudjarska I, Vornlocher HP, Zimmermann TS, Langer R, Anderson DG. A combinatorial library of lipid-like materials for delivery of RNAi therapeutics. Nat Biotechnol. 2008; 26(5):561–569. [PubMed: 18438401]

20. Faulstich H, Zobeley S, Rinnerthaler G, Small JV. Fluorescent phallotoxins as probes for filamentous actin. J Muscle Res Cell Motil. 1988; 9(5):370–383. [PubMed: 3063723]

21. Wang K, Feramisco JR, Ash JF. Fluorescent Localization of Contractile-Proteins in Tissue-Culture Cells. Methods in Enzymology. 1982; 85:514–562. [PubMed: 6750319]

22. Barber K, Mala RR, Lambert MP, Qiu RZ, MacDonald RC, Klein WL. Delivery of membrane-impermeant fluorescent probes into living neural cell populations by lipotransfer. Neuroscience Letters. 1996; 207(1):17–20. [PubMed: 8710199]

23. Bumcrot D, Manoharan M, Koteliansky V, Sah DWY. RNAi therapeutics: a potential new class of pharmaceutical drugs. Nature Chemical Biology. 2006; 2(12):711–719.

24. Kim DH, Rossi JJ. Strategies for silencing human disease using RNA interference. Nature Reviews Genetics. 2007; 8(3):173–184.

25. Lu C, Geng T, Zhan YH, Wang HY, Witting SR, Cornetta KG. Flow-through electroporation based on constant voltage for large-volume transfection of cells. Journal of Controlled Release. 2010; 144(1):91–100. [PubMed: 20117155]

Figure 1.
Microfluidic chip for electroporation. The chip has the flow channel patterned in PDMS and bonded onto a Borofloat glass slide with patterned electrodes. The electrodes extend to large contact pads for external connection. Several pairs of electrodes have been patterned for both redundancy and the ability to test different exposure times by maintaining the same flow rate and using comb structures of different widths. Insets show details of geometry and dimensions of the electrodes used in this work.
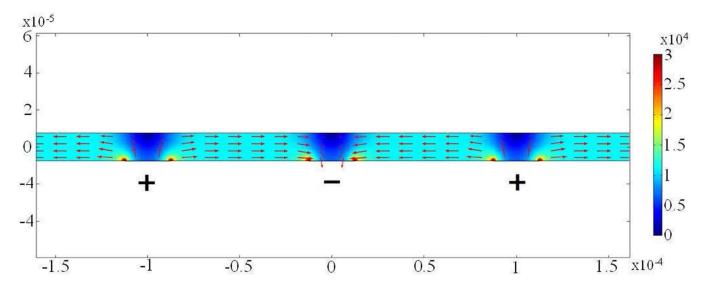
Figure 2.
Comsol simulation of the electric field in the channel with interdigitated electrodes. The figure shows the modulus of the electric field (V/m) for 1V of potential difference between the positive and negative electrodes. The system is periodic and only a portion is shown. Due to the ratio between electrode distance and channel height, the field is essentially uniform between the electrodes.
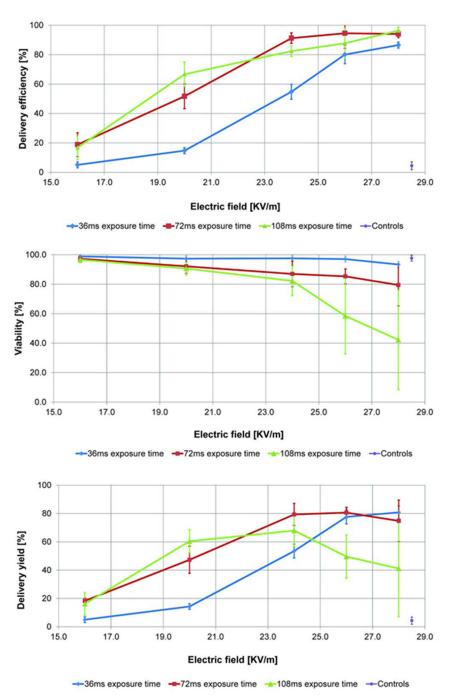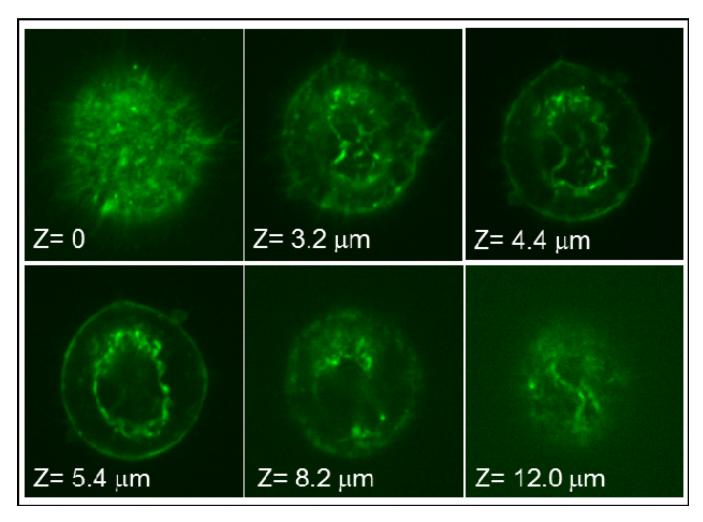
Figure 3.
Results of the flow-through electroporation of HeLa cells at 100 kHz. All of the graphs have electric field intensity in abscissa and cell exposure time to the field as a parameter. The top graph shows delivery efficiency, the middle graph shows cell viability and the bottom graph shows delivery yield. Values of delivery, viability and yield for the controls with no voltage applied are included at abscissa 28.5 kV/m. The error bars are +/− one standard deviation and each data point has been repeated at least 3 times). The experimental conditions selected are those that correspond to the highest delivery yield as identified by the first set of experiments (exposure time=72 ms, field=24 kV/m).

Figure 4.
Confocal images of a cell stained with Bodipy fluorescent phallacidin (with excitation/ emission at 505/512 nm) delivered using a field of 24 kV/m for ~72 ms. Different images refer to cross sections in different positions of the same cell. The images where collected using a filterset adequate for the Phallotoxin emission range.
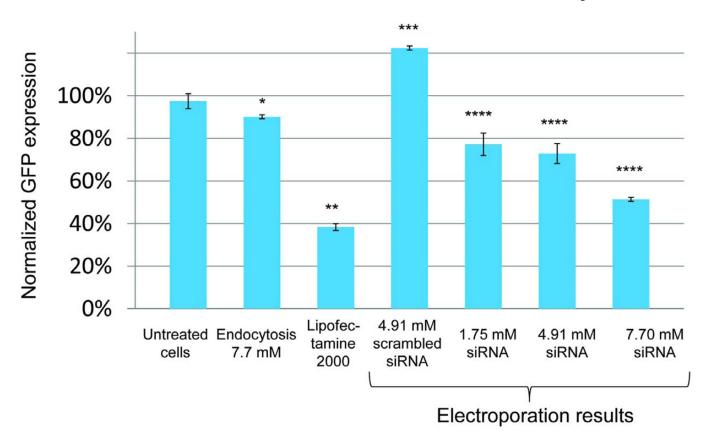
Figure 5.
GFP expression data obtained by FACS at 48 hours after treatment. Treated cells were
plated in triplicate and error bars represent one standard deviation. Observed knockdown
due to electroporation is specific and dosage dependent (**** $p < 0.001$, ANOVA with
Bonferroni post-hoc test). Scrambled siRNA does not provide gene knockdown suggesting
that electroporation itself is not responsible for the results, however it provides a difference
with the untreated cells (*** $p < 0.01$ Student's t-test with respect to untreated cells). Delivery
with standard commercial reagents such as Lipofectamine 2000 (Invitrogen, U.S.A) is
included for comparison (** $p < 0.001$ Student's t-test with respect to the untreated cells).
Endocytosis does not give a statistically significant variation of GFP expression